JOURNAL OF AGRICULTURAL AND FOOD CHEMISTRY

Article

Cite This: J. Agric. Food Chem. 2019, 67, 4603−4610

pubs.acs.org/JAFC

Detection of Pyocyanin Using a New Biodegradable SERS Biosensor Fabricated Using Gold Coated Zein Nanostructures Further Decorated with Gold Nanoparticles

Fei Jia,[†,‡] Emma Barber,[‡] Hazal Turasan,[‡] Sujin Seo,[§] Ruitong Dai,[†] Logan Liu,[§] Xingmin Li,*[,†] Arun K. Bhunia,[‡] and Jozef L. Kokini*[,‡]

[†]College of Food Science and Nutritional Engineering, China Agricultural University, Beijing, 100083, China

[‡]Department of Food Science, Purdue University, West Lafayette, Indiana 47906, United States

[§]Department of Electrical and Computer Engineering, University of Illinois at Urbana-Champaign, Urbana, Illinois 61801, United States

Supporting Information

ABSTRACT: In this paper, a biodegradable gold coated zein film surface enhanced Raman spectroscopy (SERS) platform, with gold nanoparticles (AuNPs) deposited on the surface to further enhance the Raman signal, was used to detect pyocyanin (PYO), the toxin secreted by *Pseudomonas aeruginosa*. An inverted pyramid structure imprinted on a zein film and gold coated during the transfer process was further improved with the deposition and fixing of gold nanoparticles, which resulted in enhancement of the SERS signal by approximately a decade. This new platform served as a lab-on-a-chip sensor to enable the sensitive and rapid detection of PYO in drinking water. The size, distribution, and morphology of the zein film nanostructures including the presence and distribution of gold nanoparticles were characterized by scanning electron microscopy (SEM). The new zein-based platform has the advantage of being largely biodegradable compared with commercial silicon- or glass-based platforms. The limit of detection for PYO using the newly developed zein-based SERS sensor platform was calculated as 25 μM, considerably lower than the concentration of PYO in the blood of people with cystic fibrosis which has been reported to be 70 μM.

KEYWORDS: *zein film, pyocyanin, biodegradable, SERS sensor, inverted pyramid structure*

1. INTRODUCTION

Pseudomonas aeruginosa is an opportunistic water-borne pathogen of major public health concern that can cause nosocomial infection leading to pneumonia, endocarditis, enterocolitis, and other types of infections yielding substantial medical costs and high mortality.[1] Due to the great therapeutic challenges *P. aeruginosa* brings, it is very important to develop rapid detection methods aiming at early detection and diagnosis.[2] Pyocyanin (PYO, 1-methoxy-5-methylphenazine) is the most important and lethal toxin that is released by *P. aeruginosa*. This makes PYO an excellent and unique candidate biomarker for the indirect detection of *P. aeruginosa*.[3]

Currently, high performance liquid chromatography (HPLC) and high performance liquid chromatography−mass spectrometry (HPLC−MS) based methods are the most frequently used analytical methods to detect PYO in clinical specimens.[4] Unfortunately, the high cost of the equipment and the time-consuming purification procedures needed, restrict timely detection of the toxin. Due to the redox active nature of PYO, electrochemical-based biosensors are emerging as a rapid and sensitive way to detect PYO at the point-of-care (POC).[5] Some voltammetry methods, such as cyclic voltammetry (CV),[6,7] differential pulse voltammetry (DPV),[8] and square wave voltammetry (SWV),[9] have been used to detect PYO exclusively at a negative potential around −250 to −300 mV. The disadvantage of this method is that false negative results inevitably occur, even if the redox peaks of PYO can be separated from other phenazines with similar electrochemical behavior.[10,11]

Surface enhanced Raman spectroscopy (SERS) has become a rapid and promising analytical approach with the ability to enhance Raman scattering patterns characteristic of the molecule by decorating the surface of the substrate with metal nanoparticles (usually gold or silver colloids).[12,13] As a reliable and sensitive detection method, SERS has been widely used in different fields, such as biological diagnosis, environmental monitoring, and food quality, to determine various analytes including chemical and biological hazards.[14−16] By increasing the density of "hot spots" on the SERS substrate, the SERS enhancement factor can be increased, which would also increase the sensitivity of the detection.[17,18] It is possible to create more "hot spots" either by decorating the substrate with micro/nano structures or employing nanoparticles of different size and morphology (nanocage, nanorod, nanocube, and nanosphere etc.).[19] In our previous study, we found that SERS substrate with inverted pyramid structure has the best enhancement of Raman signal compared with other structures

Received: December 31, 2018
Revised: April 3, 2019
Accepted: April 8, 2019
Published: April 9, 2019

DOI: 10.1021/acs.jafc.8b07317
J. Agric. Food Chem. 2019, 67, 4603−4610

that included positive-pyramid, nanopillar, and nanopore.[20,21] Biodegradable gold coated zein SERS substrates have been rarely studied and offer a path to protect the environment from the burden created by nonbiodegradable materials. So far, the most common SERS substrates that are commercially available are still made of nonbiodegradable materials, such as silicon or glass.

Zein is a corn protein that can be easily obtained as a byproduct of ethanol production.[22] Due to the special physical and chemical characteristics, zein proteins are mainly used as biodegradable packaging material and a protein feed supplement for animals in the traditional animal industry.[23] However, its favorable surface properties can (1) ensure the preferential adhesion of zein films with gold and (2) confer the ability to modify its surface with nanostructures such as positive pyramids, inverted pyramids, nanopillars, and nanopores[21,24] using soft lithography. These special properties make zein films a promising candidate as a biodegradable SERS platform in biosensor fabrication, instead of traditional nonbiodegradable inorganic materials. It is also pretty inexpensive and easy to capture with an ethanol extraction of DDGS (dried distiller grains with solubles) after ethanol production.

In this paper, we aim to demonstrate the feasibility of manufacturing a new biodegradable SERS biosensor consisting of our existing inverted pyramid gold coated nanostructure imprinted on zein film further improved by the deposition and fixing of gold nanoparticles on the surface of the gold film. This enabled fabrication of a novel platform for the rapid and sensitive, label-free point-of-care (POC) detection of PYO. We fabricated zein films with inverted nanopyramids coated with a 200 nm gold layer further decorated with 50 nm AuNPs fixed on the gold layer using cysteamine. It is anticipated that the number of "hot spots" will increase considerably by the contact of gold and AuNPs, especially at the bottom of the inverted pyramids and the edge areas of the inverted pyramid structures. We therefore offer an alternative biodegradable new SERS platform, which is inexpensive and eco-friendly, thereby providing an alternative to nonbiodegradable substrates used in industry. We will show how PYO in optimized conditions can be rapidly detected by using the spectral signature of PYO at 676 $cm^{-1}$and 1353 cm^{-1} using SERS with a largely biodegradable platform.

2. MATERIALS AND METHODS

2.1. Reagents and Apparatus. Pyocyanin (PYO) from *P. aeruginosa*, ≥98% (HPLC), in dimethyl sulfoxide (DMSO) was obtained from Sigma-Aldrich (St. Louis, MO, U.S.A.). Before use, a solution with a 1 mM concentration of PYO was prepared by adding appropriate amounts of ethanol and water to get a 10% ethanol solution. Then dilutions between 1 mM to 1 nM were made by subsequent 10-fold dilutions. Gold nanoparticle dispersions with a diameter of 50 nm were purchased from Ted Pella (Redding, CA, U.S.A.) and stored at 4 °C when not in use. Zein powder and cysteamine were obtained from Sigma-Aldrich (St. Louis, MO, U.S.A.). Oleic Acid was purchased from Alfa Aesar (Ward Hill, MA, U.S.A.). Monoglyceride was obtained from Caravan Ingredients (Lenexa, KS, U.S.A.).

The morphology of the zein film nanostructures was determined using a FEI Nova NanoSEM scanning electron microscope (Hillsboro, Oregon, U.S.A.) with an acceleration voltage of 10 kV. An Everhart-Thornley detector (ETD) and a through lens detector (TLD) were used to obtain images with different magnifications. The gold layer was coated on polydimethylsiloxane (PDMS) by using a Airco Temescal VES 2550 e-beam evaporator (Livermore, CA, U.S.A.). All the ultrapure water used in the experiments was obtained from a Barnstead GenPure ultrapure water purification system (Grand Island, NY, U.S.A.) and had a resistivity of 18.2 MΩ·cm^{-1}. Raman tests were conducted on a Thermo Scientific DXR2 Raman microscope (Grand Island, NY, U.S.A.). A Fisher brand Isotemp Advanced stirring hot plate was used to dissolve the zein powder (Chicago, IL, U.S.A.).

2.2. Zein/Au SERS Substrate Preparation. In order to fabricate the zein/Au SERS substrate with an inverted pyramid structure coated with gold, a previously established procedure was used.[21] Briefly, the original master molds with the inverted pyramid structures made of polyethylene terephthalate (PET) with a base of 2 μm by 2 μm, a periodicity of 2 μm (from center to center), and height of 2.1 μm were obtained from the Dr. Liu's laboratory at the University of Illinois. Then PDMS was used to transfer the microphotonic patterns and gold from PET to the zein film. Zein films were cast on the PDMS molds following the procedure below: Zein solution was prepared by dissolving zein powder in 70% ethanol, oleic acid (plasticizer), and monoglyceride (emulsifier) together. First, 100 mL of ethanol (70%) was heated to 65 °C and 20 g of zein powder was added to the heated ethanolic solution. After zein was dissolved for 5 min under stirring, 20 g of oleic acid and 0.1 g of monoglyceride were added to the solution. Air bubbles were removed by 2 min of sonication immediately after the mixing of zein, plasticizer, and emulsifier to make bubble free zein films. Afterward, 15 mL of the zein solution was poured into a Petri dish containing the PDMS-Au mold in the middle. Then the solution was dried in a desiccator for 3 weeks at room temperature. Finally, zein films were cut carefully by using a razor blade after complete solidification. The surface energy of gold on PDMS is lower than the surface energy of gold on zein, and therefore, the gold spontaneously and flawlessly transfers onto the zein film. The zein/Au film with three-dimensional inverted pyramid structure was peeled from PDMS and the final gold coated zein nanophotonic SERS substrate was obtained.

2.3. AuNP Decoration of the Surface of the Zein/Au Substrate. Once the gold coated zein sensors were fabricated, the effect of using gold nanoparticles to further increase the SERS intensity was investigated. Cysteamine was used as a cross-linker to bind the gold nanoparticles that decorate the surface of the SERS sensors. First, a 1 M cysteamine solution was prepared using milli-Q water. The 1 M solution was then diluted to both 10 mM and 100 mM cysteamine. Concentrations a decade apart were selected to have a large enough difference so that the impact of cysteamine on gold density could easily be established. These cysteamine concentrations were explored for their ability to create a uniform monolayer of gold nanoparticles and for the effect of cysteamine concentration on the density of gold nanoparticles.

A 25 μL droplet of 10 mM or 100 mM cysteamine was placed on the surface of the gold coated zein sensor. This droplet size was enough to cover the portion of the sensor containing the inverted micropyramids in its entirety for both 10 mM and 100 mM cysteamine concentrations. The sensor was covered and left at room temperature for 2 h to allow for the cysteamine to form its own monolayer. The sensors were then washed using milli-Q water and dried with a stream of nitrogen gas.

A 25 μL droplet of a 4.5×10^{10} particle/mL solution of 50 nm gold nanoparticle (NP) solution was then placed on the zein sensor again, over the inverted nanoparticles. The sensor was placed in a Petri dish, covered, and sealed with parafilm before being placed in the refrigerator at a temperature of 4 °C for 20 h. The sensors were then washed again with milli-Q water and dried with nitrogen gas. The subsequent sensors emerged from this process decorated with gold nanoparticles, and the different concentrations of cysteamine were investigated for their ability to enhance the zein SERS signal.

2.4. Enhancement Factor of the SERS Substrate. Raman tests were conducted by measuring the Raman spectra on the substrate in different positions (with the inverted pyramid structure and without the structure) and different conditions (coated with AuNPs and without AuNPs) of the SERS substrate. In these experiments, zein peaks were used as the basis for understanding the enhancement factor.

DOI: 10.1021/acs.jafc.8b07317
J. Agric. Food Chem. 2019, 67, 4603−4610

Additional experiments were also performed using Rhodamine 6G (R6G) as the analyte to test the Raman signal intensity. The zein SERS sensors compared were: (1) with no Au coating layer on zein, (2) with no Au nanoparticles deposited on the gold layer, (3) with Au nanoparticles deposited and bound on the gold layer using 10 mM cysteamine, and (4) with Au nanoparticles deposited and bound on the gold layer using 100 mM cysteamine.

Raman spectra were collected using a Thermo Scientific DXR2 Raman microscope. The 633 nm laser was used at a power of 2 mW with a long working distance 50× objective lens. The laser power was optimized to get the highest intensity signal from the sample without saturating the detector. In conjunction with a 25 μm pinhole aperture, this lens created a total laser spot size of 1.3 μm. This aperture was chosen from four available apertures (25 μm pinhole, 25 μm slit, 50 μm pinhole, and 50 μm slit) to give the highest possible intensity from the sample without having truncated peaks due to saturation of the detector. In this particular case, the 25 μm pinhole aperture gave the highest intensity without peak truncation. Atlμs software was used to perform *xy*-mapping of the sensor. Each map was a 6 × 6 μm square with a 2 μm step size in each direction, creating a total of 9 points captured for each map. This distance ensured that the laser focus was at the center of an inverted pyramid for each collection.

Every sample was photo bleached for 20 s before collecting a spectrum to decrease the fluorescence caused by the zein protein. The spectra were collected from 200 to 3600 cm^{-1}. All 9 spectra collected from each map were averaged together and then manually baseline corrected to remove any interference from zein fluorescence. Five maps were collected for each of the sensors tested, totaling 45 spectra collected for each sensor and 135 spectra for each formulation.

2.5. Determination of PYO Concentration on the New Zein/Au-AuNPs SERS Platform. Twenty microliter portions of different concentrations of PYO in a DMSO buffer with 10% ethanol (ranging from 50 μM to 1 mM) and the blank buffer solution without PYO were dropped at the center of the zein/Au-AuNPs substrate (prepared using 100 mM cysteamine). A 633 nm laser was used as the laser source. The slit selected was 50 μm, and the grating used was 600 lines/mm. In contrast to the experiments above, of the four aperture choices that were available on this Raman instrument, the 50 μm slit aperture was used and gave the best peak without peak truncation and maximum intensity. The wavenumber ranges between 600 and 2000 cm^{-1} were recorded. Spectra were collected 10 times for a period of 1 s. *X-Y* Mapping was used to collect data on a 30 μm by 30 μm square.

2.6. Test in Drinking Water. The effectiveness of the zein sensor platform was investigated with tap water spiked with PYO. In order to eliminate possible big particles such as plankton and suspended dust, the water was allowed to rest for 30 min in order to detect possible precipitated particles. These possible microparticles were removed by centrifugation for 30 min at 14000 rpm. The supernatant was then further filtered (0.2 μm filter pore size) to remove any possible smaller microaggregates.

Three different concentrations of the PYO solution (500 μM, 1 mM, and 2 mM) were prepared for addition to the treated water sample by mixing 0.9 mL of water with 0.1 mL of standard PYO solution. A drop of the PYO solution in water was deposited on the surface of the zein/Au-AuNPs SERS sensor. Raman spectroscopy measurements were conducted in triplicate.

2.7. Biodegradability and Gold Recovery from the Biosensor. To test the biodegradability of the zein/Au-AuNPs SERS substrate, recovery experiments were conducted by using 20 mL of 70% ethanol extraction to separate zein from gold. The biodegradable sensors were put into the ethanol solution on a magnetic stirrer with 700 rpm at room temperature and 65 °C, respectively. Afterward, gold material was filtered from the solution. The remaining gold free zein ethanol solution was disposed of by Purdue University Radiological and Environmental Management (REM).

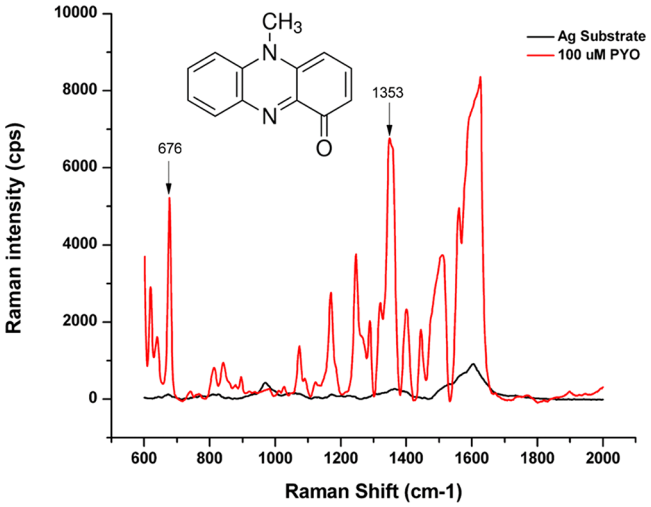

Figure 1. Chemistry of PYO and the standard Raman spectrum of PYO measured using Ag as a SERS substrate (red line).

3. RESULTS AND DISCUSSION

3.1. Detection Mechanism. As seen Figure 1, PYO is made of heterocyclic nitrogen with a methyl group at the N position. The Raman spectrum of 100 μM PYO using commercially available 20 nm silver nanoparticles (AgNPs) as a SERS substrate gives characteristic peaks between 650 and 1600 cm^{-1} compared with pristine Ag. Three prominent peaks, at 676, 1353, and 1610 cm^{-1}, are observed originating from PYO. The peaks at around 850 and 1080 cm^{-1} are attributed to the molecular vibrations of ethanol. The Raman peak of 1353 cm^{-1} was assigned to C−C stretching, C−N stretching, and C−H in-plane bending modes of the aromatic ring.[25] The spectral peak at 1447 cm^{-1}, is the result of the CH_2 and CH_3 bending. In this study, we are using the 676 and 1353 cm^{-1} peaks as markers of PYO to detect and determine the concentration of PYO in the sample.

3.2. Fabrication Principle and Sensing Strategy. The basic fabrication principle and detection mechanism of the SERS nanosensor can be seen in Figure 2. The three steps needed to develop the nanosensor include fabricating the PDMS intermediate followed by zein substrate fabrication and PYO detection. The gold coated zein nanophotonic film was developed as in earlier studies.[21] AuNPs to enhance the SERS signal were attached to the surface of the gold coated zein film. A 100 mM solution of the cross-linker, cysteamine, was used to ensure bonding between the AuNPs and the gold film on the surface of zein.

Raman measurements are then conducted by depositing a drop of PYO solution on the SERS substrate consisting of the gold coated zein film with AuNPs (part III in Figure 2). There is then an enhancement of the Raman spectrum intensity of the PYO solution as a function of the concentration of PYO deposited by the drop. The change in the intensity of the SERS signal as a function of concentration was used to quantitatively detect PYO.

3.3. Characterization of the Zein/Au Substrate. The SEM images of the zein substrates with no Au layer and no NPs (Figure 3a) show that a successful transfer of the inverted micropyramids was achieved through soft lithography using PDMS as the intermediate mold. Figure 3b shows the zein film coated with a 200 nm Au layer. It is clear that the inverted pyramid structure and the nonstructure sections are distinctly

DOI: 10.1021/acs.jafc.8b07317
J. Agric. Food Chem. 2019, 67, 4603−4610

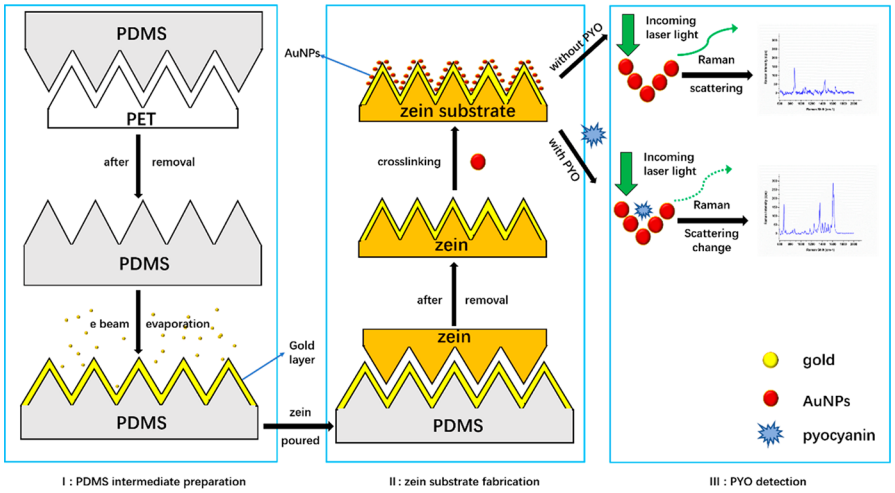

Figure 2. Fabrication of the zein substrate and sensing strategy using the SERS biosensor.

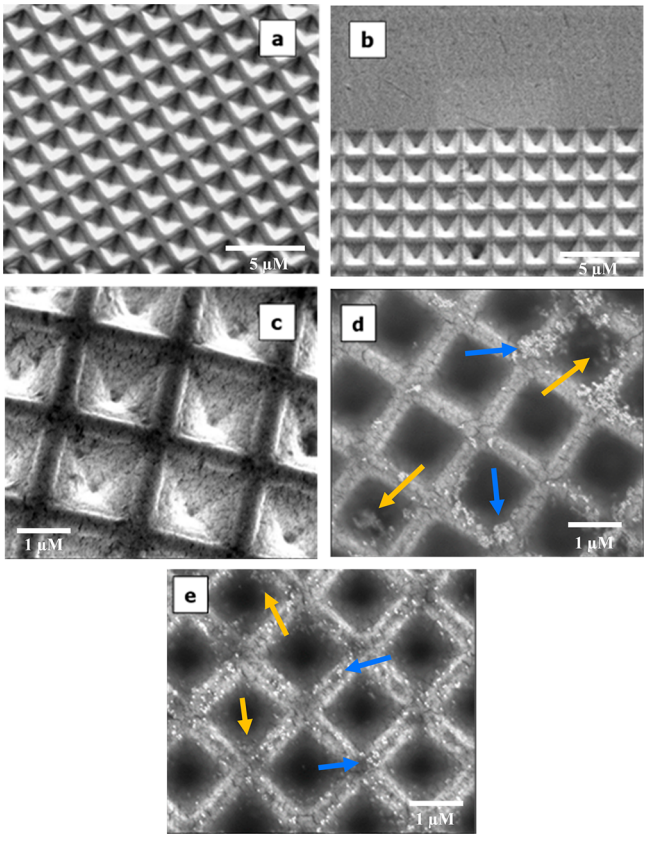

Figure 3. Characterization of the inverted pyramid structure in each step of the zein film fabrication: (a) no Au and no AuNPs on the zein film, (b) gold coated zein film captured by an Everhart-Thornley detector (ETD), (c) gold coated zein film captured by the Through Lens detector (TLD), (d) gold coated and AuNPs functionalized zein film using 10 mM cysteamine, and (e) gold coated and AuNPs functionalized zein film using 100 mM cysteamine. Yellow arrows show AuNPs in the inverted pyramid wells, and blue arrows show AuNPs on top of the wells.

seen. The upper area in Figure 3b is the zein film without inverted pyramid structure showing a smooth and clean zein surface without pyramids. The lower area in Figure 3b shows the well-organized inverted pyramid structure distributed uniformly on the surface.

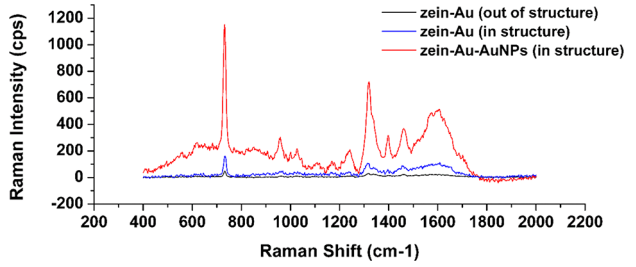

Figure 4. Raman spectra of zein/Au substrate (without inverted pyramid structure), zein/Au (measured in the inverted pyramid structure), and zein/Au-AuNPs (measured in the area with the inverted pyramid structure).

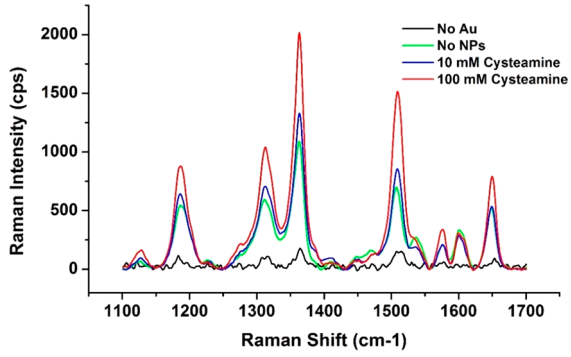

Figure 5. Raman spectra of zein SERS platforms with Rhodamine 6G analyte: no Au (black), no NPs (green), 10 mM cysteamine (blue), and 100 mM cysteamine (red).

The inverted pyramid structures can be observed clearly by the ultrasensitive immersion mode and in detail in Figure 3c. Each inverted pyramid has lateral base dimensions of 2 μm by 2 μm with a periodicity of 2.1 μm, which matched perfectly the positioning of the pyramids on the PET mold.

The SEM comparison of the AuNP bound to the surface of the gold coated nanostructured zein film using 100 mM and the 10 mM cysteamine solutions showed that a much denser dispersion of nanoparticles was achieved with the 100 mM cysteamine solution compared to the 10 mM solution (Figure 3d,e). The 10 mM concentration of cysteamine succeeded in attaching a considerable number of gold nanoparticles to the sensor surface, but they were not evenly distributed. The

DOI: 10.1021/acs.jafc.8b07317
J. Agric. Food Chem. 2019, 67, 4603−4610

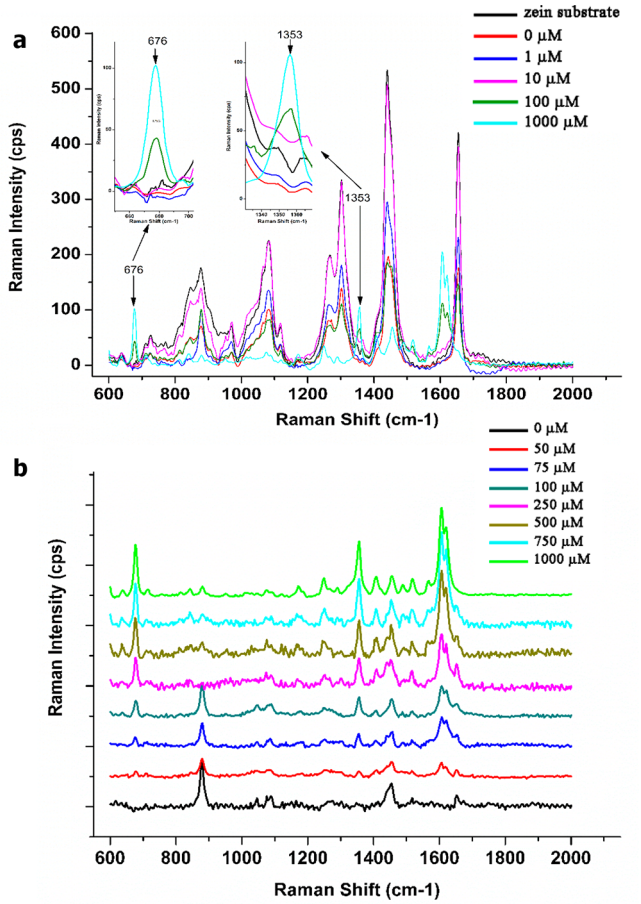

Figure 6. (a) Raman spectra of zein/Au-AuNPs substrate in detecting different concentrations of PYO ranging from 1 to 1000 μM. (b) Raman intensity change along with the increase of PYO concentration from 50 to 1000 μM.

nanoparticles mostly congregated in a few areas throughout the sensor surface. The large aggregates of gold NPs on the 10 mM cysteamine samples appeared to be mainly located at the top of the inverted micropyramids. This placement is not ideal, as the signal could be more enhanced if a considerable fraction of the particles were stacked up at the bottom of the inverted pyramid wells.

The 100 mM solution of cysteamine was able to achieve a good dispersion of gold nanoparticles across the whole sensor surface. Particles were present both within the wells of the inverted pyramids as well as toward the top between the wells. Therefore, the distribution of the nanoparticles with the 100 mM cysteamine sample provided a SERS signal of much greater intensity.

3.4. Relative SERS Enhancement with the Newly Fabricated Gold Coated AuNPs Decorated Sensor Platform. Figure 4 shows the results of Raman measurements at different locations of the zein SERS platforms (with and without inverted pyramid structure) and the same area with different gold decoration conditions (with and without AuNPs) under the same Raman setting parameters. The blue line is the Raman spectrum of the 200 nm gold coated zein platform with the inverted pyramid microstructure ,and the black line is the Raman spectrum of the same platform measured in the area without the inverted pyramid microstructure. The Raman signal of the two lines at the wavelength of 731 cm^{-1} generated by the zein protein, which is not particularly Raman active, gave a signal with intensities around 200 cps (counts per second) for the blue line and 100 cps for the black line showing that the gold coated inverted pyramid structure improves the Raman signal considerably.[21] The red line shows the Raman spectrum of the gold coated zein substrate decorated with AuNPs which gives a Raman signal around 1200 cps for the 731 cm^{-1} zein peak, which is 5 times higher compared to the blue spectrum. The enhancement of the Raman signal showed that the introduction of AuNPs to the substrate significantly increases the Raman response. The contact of AuNPs and the gold layer creates a large number of "hot spots", which contribute to the enhancement of the Raman signal.[26] To achieve the best sensitivity of the nanosensor, we use the 100 mM cysteamine zein/Au-AuNPs which maximize the enhancement of the SERS platform to detect PYO.

The enhancement of the SERS signal with different surface preparations was then tested using the Raman active molecule Rhodamine 6G (R6G) as the target analyte. The R6G peak intensity at 1360 cm^{-1} was measured as a reference of each sensor's enhancement. This peak is indicative of the aromatic ring vibrations that are highly present in the R6G molecule but are not present in the zein molecular structure. As shown in Figure 5, the AuNP decorated sensor had the strongest Raman signal overall, and the Raman intensity of the R6G peak at 1360 cm^{-1} is around 2016 cps. The intensity of the zein spectrum without any gold (No Au), however, was very small (176 cps) compared to the gold coated zein substrate (1089 cps). The SERS enhancement factor calculation is then given as follows for the gold decorated gold coated zein substrate[21]

$$\text{enhancement factor} = \frac{I_{\text{SERS}}}{I_{\text{Raman}}} \times \frac{C_{\text{Raman}}}{C_{\text{SERS}}} \times \frac{A_{\text{SERS}}}{A_{\text{Raman}}}$$

where I_{SERS}, C_{SERS}, and A_{SERS} represent the SERS intensity, the concentration of Rhodamine 6G, and the surface area covered by Rhodamine 6G molecules, respectively. Similarly, I_{Raman}, C_{Raman}, and A_{Raman} represent the Raman intensity, concentration of Rhodamine 6G, and the surface area covered by Rhodamine 6G molecules, respectively. The SERS enhancement of the gold coated (200 nm thickness) nanostructured zein platform without any gold nanoparticles has been previously calculated as 1.3×10^4.[21] To calculate the additional SERS enhancement achieved by the gold nanoparticle decoration, the surface area generated by the gold nanoparticles from the gold nanoparticle colloid concentration and the volume of gold nanoparticles used was calculated. The Raman intensity improvement generated through the use of gold nanoparticles is also calculated. Multiplication of these two factors with the previously obtained SERS enhancement gave an improved SERS enhancement factor of 2.8×10^4.

Some of the inverted nanoparticle wells had no particles while others had a considerable number, creating a similar spectrum to the no NPs platform in the former case and a largely enhanced signal in the latter. Clearly, the Raman spectra showed that the zein sensor platform coated with gold and decorated with gold nanoparticles was the better platform. This sensor setup was further tested for detection of the PYO.

3.5. Detection Ability of the SERS Nanosensor for PYO. The results of the Raman tests to detect PYO at different concentrations from 0 to 1000 μM are in Figure 6a, where we can see the characteristic peaks of 676 and 1353 cm^{-1} of PYO. At the concentration of 1000 μM, large PYO Raman peaks

DOI: 10.1021/acs.jafc.8b07317
J. Agric. Food Chem. 2019, 67, 4603−4610

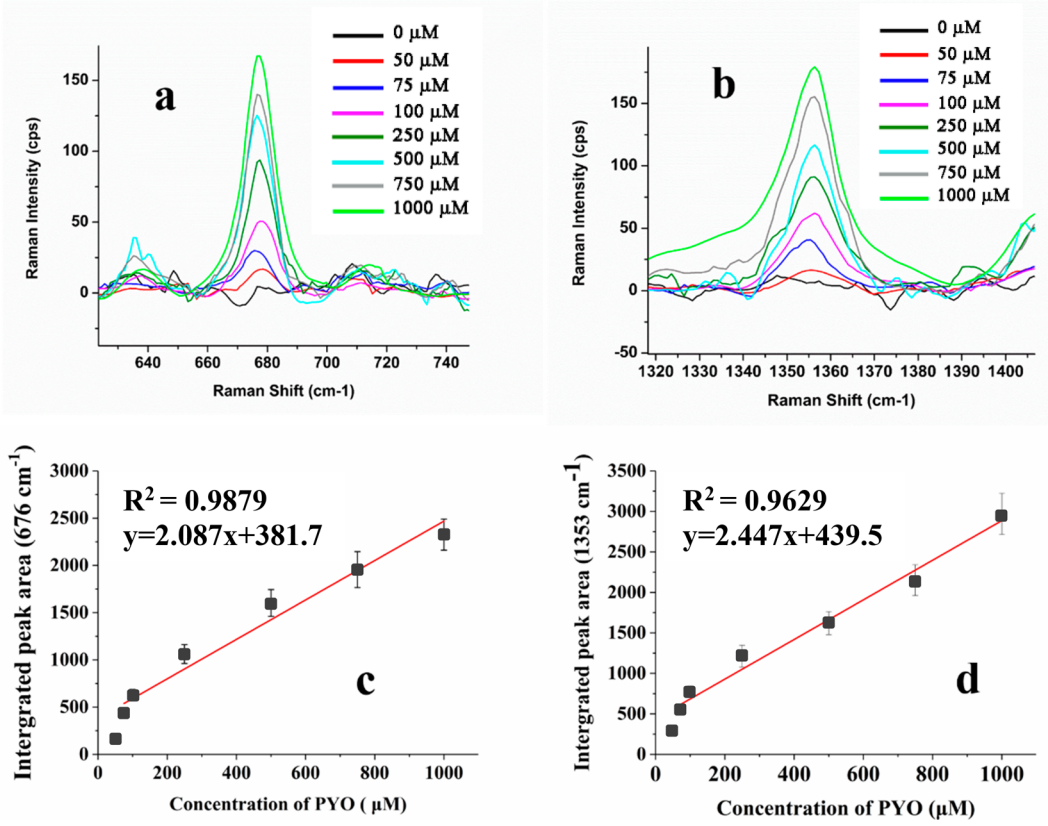

Figure 7. Raman spectra of zein/Au-AuNPs substrate in detecting different concentrations of PYO ranging from 50 to 1000 μM (a and b) and the standard curve of the SERS sensor in detecting different concentrations of PYO ranging from 50 to 1000 μM (c and d) at 676 and 1353 cm^{-1}.

Table 1. Recovery of PYO in Drinking Water Samples Using Developed SERS Nanosensor (n = 3)

Water Sample number	Spiked concentration (μM)	Measured concentration by SERS (μM)	Recovery (%)
Water 1	50.00	46.31 ± 0.66	92.62
Water 2	100.00	98.09 ± 0.48	98.09
Water 3	200.00	190.8 ± 1.57	95.40

appeared, while at 10 μM and below, there is no peak at the two characteristic wavenumbers. We deduced that the critical concentration of PYO for adequate detection should be between 10 and 100 μM. Figure 6b shows the Raman intensity changes of the characteristic peaks as a function of PYO concentration from 50 to 1000 μM. A 10% ethanol/water solution which was used to dilute PYO concentration and served as a control showed no Raman peaks at the wavelengths of 676 and 1353 cm^{-1} in Figure 6a as expected. However, peaks began to appear when the PYO concentration reached 50 μM and showed an increasing Raman intensity when the concentration of PYO increased to 100 μM.

In order to further quantify the analysis, two calibration curves were developed for PYO at the characteristic peaks of 676 and 1353 cm^{-1} at different concentrations of PYO ranging from 50 to 1000 μM. More detailed peak intensity information on the Raman spectra can be obtained by enlarging the spectra (Figure 6b). Figure 7a shows the Raman 676 cm^{-1}peak of PYO. A Raman peak with an intensity of 20 is observed when the concentration of PYO is 50 μM and the area underneath the peak appears to increase linearly from 75 to 1000 μM giving a standard curve, with an equation of $y = 2.087x + 381.7$, using the change in peak areas as a function of concentration as shown in Figure 7c. The coefficient of determination, R^2, for this calibration curve is 0.9879. A similar linear equation of $y = 2.447x + 439.5$ with an R^2 of 0.9629 was obtained at the wavelength of 1353 cm^{-1} (Figures 7b,d). The limit of detection (LOD) of 25 μM was calculated at this wavenumber according to the formula LOD = 3N/S.

Pyocyanin is found in the sputum of patients with cystic fibrosis in concentrations as high as 16 μg/mL corresponding to 0.07 μmol/mL and has many toxic effects on eukaryotic cells, including the respiratory epithelium.[27] In our current biosensor, the LOD was found to be 25 μmol/L corresponding to 0.025 μmol/mL. While there may be sensors with much higher sensitivity, the biodegradable nature of our sensor offers a different benefit coupled with a sensitivity which is in the range where damaging impact is observed on the part of pyocyanin. When other SERS-based nanosensors and the sensor in this paper for PYO detection are considered, we can see that the LOD of each nanosensor varies a lot with different nanomaterials used in the construction of the sensor and different characteristics peaks used.[25,28−30] The ultrahigh Raman enhancement factor on Au@SiO_2 supercrystal arrays for PYO gives the best limit of detection of 10^{-14} M in PYO detection.[30] Some silver nanoparticle-based fabricated SERS nanosensors can also test PYO to a very low level successfully[25,29] (for detailed comparison between LODs of SERS PYO studies see Table S-1). However, in this research, we have shown that a reliable and biodegradable sensor can be fabricated. The measurements were taken from three independently fabricated sensors, and the outcome is a marker of the reproducibility of the method used with the standard

DOI: 10.1021/acs.jafc.8b07317
J. Agric. Food Chem. 2019, 67, 4603−4610

deviation showing the variability from sensor to sensor. The sensor platform is also very stable. Our research on sequentially improvement platforms has been going for more than 8 years at this time. The early sensors manufactured in our lab still give good reproducibility showing the stability of our platforms. The zein-based sensor is the only platform that is biodegradable among all the platforms studied so far and exhibits great advantages over the conventional inorganic material-based chips in terms of protecting the environment in an age of exponential growth in the development and commercialization of point-of-care sensors.

3.6. SERS Detection of PYO in Drinking Water. In order to validate our methodology, a relevant water safety application is considered in this study. A PYO recovery experiment from drinking water was used to evaluate the feasibility and reliability of the PYO bionanosensor. The peak area at 676 cm^{-1} was used to calculate the concentration of PYO detected in drinking water. As shown in Table 1, the recovery rates between 92.62% and 98.09% showed good capabilities of the nanosensor in this study for accurate PYO detection in drinking water.

3.7. Biodegradability Test. It is known that zein is an alcohol soluble protein, and one of the best solvents for zein is a 70% ethanol solution. We immersed our sensors in 70% ethanol and extracted the zein and the gold separately. In the extraction experiments, we can see clearly that the zein/Au-AuNPs substrate can be completely dissolved in the 70% ethanol solution. It takes 4.5 h for the substrate to reach 100% dissolution at room temperature. Heat can accelerate the dissolution of zein in 70% ethanol. The SERS substrate was totally dissolved at 65 °C within less than 1 h. The gold material can be harvested easily by filtration (see Figure S-1).

In short, a new promising biodegradable SERS platform made of gold coated nanostructured zein decorated with 50 nm gold nanoparticles was fabricated, which successfully detected PYO secreted by *P. aeruginosa*. The new platform gave a SERS enhancement factor of 2.8×10^4 and successfully enhanced the Raman intensity of PYO. PYO can be quantified in 30 min directly without complex pretreatment, and this platform was used to detect PYO in PYO spiked drinking water. This point-of-care detection method for PYO can be further used for on-site detection of PYO in drinking water or beverages that are suspected to be contaminated with *P. aeruginosa*. The zein-based substrate, which was very easy to reclaim using ethanol extraction, is biodegradable and eco-friendly. Gold can be harvested and further used once the sensor has been used and discarded. Recycling silicone involves depolymerization to recover silicone monomers, which is a time and energy consuming process.[31] Glass is inert, but it does not biodegrade in the environment.[32] Consequently, the use of zein is a far superior platform from an environmental point of view.

■ ASSOCIATED CONTENT

Supporting Information

The Supporting Information is available free of charge on the ACS Publications website at DOI: 10.1021/acs.jafc.8b07317.

A comparison of studies conducted for the determination of *P. aeruginosa* including our study, details of biodegradability test conducted on the zein sensor platforms for recovery of gold layer (PDF)

■ AUTHOR INFORMATION

Corresponding Authors

*Phone: 765-494-8256. E-mail: jkokini@purdue.edu.
*Phone: +86-010-62737547. Fax: +86-010-62737547. E-mail: lixingmin@cau.edu.cn.

ORCID

Jozef L. Kokini: 0000-0003-4048-8891

Notes

The authors declare no competing financial interest.

■ ACKNOWLEDGMENTS

Fei Jia was supported by the Beijing Innovation Consortium of Agricultural Research System (BAIC04-2018). The research was supported by the Scholle Endowment Foundation of Purdue University.

■ REFERENCES

(1) Buzid, A.; Muimhneacháin, E. Ó.; Reen, F. J.; Hayes, P. E.; Pardo, L. M.; Shang, F.; O'Gara, F.; Sperry, J.; Luong, J. H. T.; Glennon, J. D.; et al. Synthesis and Electrochemical Detection of a Thiazolyl-Indole Natural Product Isolated from the Nosocomial Pathogen Pseudomonas Aeruginosa. *Anal. Bioanal. Chem.* **2016**, *408* (23), 6361−6367.

(2) Baig, N.; Polisetti, S.; Morales-Soto, N.; Dunham, S. J. B.; Sweedler, J. V.; Shrout, J. D.; Bohn, P. W. Label-Free Molecular Imaging of Bacterial Communities of the Opportunistic Pathogen Pseudomonas Aeruginosa. In *Biosensing and Nanomedicine IX*; SPIE, 2016; Vol. *9930*, p 993004. DOI: 10.1117/12.2236695.

(3) Pastells, C.; Pascual, N.; Sanchez-Baeza, F.; Marco, M.-P. Immunochemical Determination of Pyocyanin and 1-Hydroxyphenazine as Potential Biomarkers of Pseudomonas Aeruginosa Infections. *Anal. Chem.* **2016**, *88* (3), 1631−1638.

(4) Yong, Y.-C.; Wu, X.-Y.; Sun, J.-Z.; Cao, Y.-X.; Song, H. Engineering Quorum Sensing Signaling of Pseudomonas for Enhanced Wastewater Treatment and Electricity Harvest: A Review. *Chemosphere* **2015**, *140*, 18−25.

(5) Yang, Y.; Yu, Y.-Y.; Wang, Y.-Z.; Zhang, C.-L.; Wang, J.-X.; Fang, Z.; Lv, H.; Zhong, J.-J.; Yong, Y.-C. Amplification of Electrochemical Signal by a Whole-Cell Redox Reactivation Module for Ultrasensitive Detection of Pyocyanin. *Biosens. Bioelectron.* **2017**, *98*, 338−344.

(6) Alatraktchi, F. A.; Breum Andersen, S.; Krogh Johansen, H.; Molin, S.; Svendsen, W. E. Fast Selective Detection of Pyocyanin Using Cyclic Voltammetry. *Sensors* **2016**, *16* (3), 408.

(7) Alatraktchi, F. A.; Noori, J. S.; Tanev, G. P.; Mortensen, J.; Dimaki, M.; Johansen, H. K.; Madsen, J.; Molin, S.; Svendsen, W. E. Paper-Based Sensors for Rapid Detection of Virulence Factor Produced by Pseudomonas Aeruginosa. *PLoS One* **2018**, *13* (3), No. e0194157.

(8) Webster, T. A.; Goluch, E. D. Electrochemical Detection of Pyocyanin in Nanochannels with Integrated Palladium Hydride Reference Electrodes. *Lab Chip* **2012**, *12* (24), 5195−5201.

(9) Webster, T. A.; Sismaet, H. J.; Conte, J. L.; Chan, I. J.; Goluch, E. D. Electrochemical Detection of Pseudomonas Aeruginosa in Human Fluid Samples via Pyocyanin. *Biosens. Bioelectron.* **2014**, *60*, 265−270.

(10) Yong, Y.-C.; Yu, Y.-Y.; Li, C.-M.; Zhong, J.-J.; Song, H. Bioelectricity Enhancement via Overexpression of Quorum Sensing System in Pseudomonas Aeruginosa-Inoculated Microbial Fuel Cells. *Biosens. Bioelectron.* **2011**, *30* (1), 87−92.

(11) Li, S. H.; Mou, Q. Q.; Feng, N. Z.; Leung, P. H. M. A Selective Medium for Pyocyanin-Dependent Fast Electrochemical Detection of Pseudomonas Aeruginosa in Environmental Microbial Samples. *Int. J. Electrochem. Sci.* **2018**, *13* (4), 3789−3798.

(12) Yoon, J.; Choi, N.; Ko, J.; Kim, K.; Lee, S.; Choo, J. Highly Sensitive Detection of Thrombin Using SERS-Based Magnetic Aptasensors. *Biosens. Bioelectron.* **2013**, *47*, 62−67.

DOI: 10.1021/acs.jafc.8b07317
J. Agric. Food Chem. 2019, 67, 4603−4610

(13) Liao, W.; Lu, X. Determination of Chemical Hazards in Foods Using Surface-Enhanced Raman Spectroscopy Coupled with Advanced Separation Techniques. *Trends Food Sci. Technol.* **2016**, *54*, 103−113.
(14) Boardman, A. K.; Wong, W. S.; Premasiri, W. R.; Ziegler, L. D.; Lee, J. C.; Miljkovic, M.; Klapperich, C. M.; Sharon, A.; Sauer-Budge, A. F. Rapid Detection of Bacteria from Blood with Surface-Enhanced Raman Spectroscopy. *Anal. Chem.* **2016**, *88* (16), 8026−8035.
(15) Sadeghi, R.; Rodriguez, R. J.; Yao, Y.; Kokini, J. L. Advances in Nanotechnology as They Pertain to Food and Agriculture: Benefits and Risks. *Annu. Rev. Food Sci. Technol.* **2017**, *8* (1), 467−492.
(16) Driver, M.; Li, Y.; Zheng, J.; Decker, E.; Julian McClements, D.; He, L. Fabrication of Lipophilic Gold Nanoparticles for Studying Lipids by Surface Enhanced Raman Spectroscopy (SERS). *Analyst* **2014**, *139* (13), 3352−3355.
(17) Zheng, J.; He, L. Surface-Enhanced Raman Spectroscopy for the Chemical Analysis of Food. *Compr. Rev. Food Sci. Food Saf.* **2014**, *13* (3), 317−328.
(18) Zheng, J.; Pang, S.; Labuza, T. P.; He, L. Evaluation of Surface-Enhanced Raman Scattering Detection Using a Handheld and a Bench-Top Raman Spectrometer: A Comparative Study. *Talanta* **2014**, *129*, 79−85.
(19) Yang, Y.; Tanemura, M.; Huang, Z.; Jiang, D.; Li, Z.-Y.; Huang, Y.; Kawamura, G.; Yamaguchi, K.; Nogami, M. Aligned Gold Nanoneedle Arrays for Surface-Enhanced Raman Scattering. *Nanotechnology* **2010**, *21* (32), 325701.
(20) Gezer, P. G.; Liu, G. L.; Kokini, J. L. Development of a Biodegradable Sensor Platform from Gold Coated Zein Nanophotonic Films to Detect Peanut Allergen, Ara H1, Using Surface Enhanced Raman Spectroscopy. *Talanta* **2016**, *150*, 224−232.
(21) Gezer, P. G.; Hsiao, A.; Kokini, J. L.; Liu, G. L. Simultaneous Transfer of Noble Metals and Three-Dimensional Micro- and Nanopatterns onto Zein for Fabrication of Nanophotonic Platforms. *J. Mater. Sci.* **2016**, *51* (8), 3806−3816.
(22) Luecha, J.; Sozer, N.; Kokini, J. L. Synthesis and Properties of Corn Zein/Montmorillonite Nanocomposite Films. *J. Mater. Sci.* **2010**, *45* (13), 3529−3537.
(23) Navdeep; Banipal, T. S.; Kaur, G.; Bakshi, M. S. Nanoparticle Surface Specific Adsorption of Zein and Its Self-Assembled Behavior of Nanocubes Formation in Relation to On-Off SERS: Understanding Morphology Control of Protein Aggregates. *J. Agric. Food Chem.* **2016**, *64* (3), 596−607.
(24) Turasan, H.; Kokini, J. L. Advances in Understanding the Molecular Structures and Functionalities of Biodegradable Zein-Based Materials Using Spectroscopic Techniques: A Review. *Biomacromolecules* **2017**, *18* (2), 331−354.
(25) Wu, X.; Chen, J.; Li, X.; Zhao, Y.; Zughaier, S. M. Culture-Free Diagnostics of Pseudomonas Aeruginosa Infection by Silver Nanorod Array Based SERS from Clinical Sputum Samples. *Nanomedicine* **2014**, *10* (8), 1863−1870.
(26) Seo, S.; Chang, T.-W.; Liu, G. L. 3D Plasmon Coupling Assisted Sers on Nanoparticle-Nanocup Array Hybrids. *Sci. Rep.* **2018**, *8* (1), 3002.
(27) Noto, M. J.; Burns, W. J.; Beavers, W. N.; Skaar, E. P. Mechanisms of Pyocyanin Toxicity and Genetic Determinants of Resistance in Staphylococcus Aureus. *J. Bacteriol.* **2017**, *199* (17), e00221−17.
(28) Nguyen, C. Q.; Thrift, W. J.; Bhattacharjee, A.; Ranjbar, S.; Gallagher, T.; Darvishzadeh-Varcheie, M.; Sanderson, R. N.; Capolino, F.; Whiteson, K.; Baldi, P.; et al. Longitudinal Monitoring of Biofilm Formation via Robust Surface-Enhanced Raman Scattering Quantification of Pseudomonas Aeruginosa-Produced Metabolites. *ACS Appl. Mater. Interfaces* **2018**, *10* (15), 12364−12373.
(29) Zukovskaja, O.; Jahn, I. J.; Weber, K.; Cialla-May, D.; Popp, J. Detection of Pseudomonas Aeruginosa Metabolite Pyocyanin in Water and Saliva by Employing the SERS Technique. *Sensors* **2017**, *17* (8), 1704.
(30) Bodelón, G.; Montes-García, V.; López-Puente, V.; Hill, E. H.; Hamon, C.; Sanz-Ortiz, M. N.; Rodal-Cedeira, S.; Costas, C.; Celiksoy, S.; Pérez-Juste, I.; et al. Detection and Imaging of Quorum Sensing in Pseudomonas Aeruginosa Biofilm Communities by Surface-Enhanced Resonance Raman Scattering. *Nat. Mater.* **2016**, *15* (11), 1203−1211.
(31) HARMONY INDUSTRIES INC. | HOME http://www.harmonyrecycling.com/silicone_rubber_recycling.html (accessed Mar 6, 2019).
(32) Center for Microbial Oceanography, Mote Marine Laboratory. Survey of Underwater Plastic and Ecosystem Response Cruise: Marine Debris Biodegration Time Line http://cmore.soest.hawaii.edu/cruises/super/biodegradation.htm (accessed Mar 7, 2019).

DOI: 10.1021/acs.jafc.8b07317
J. Agric. Food Chem. 2019, 67, 4603−4610